Development 133, 2865-2874 (2006) doi:10.1242/dev.02478

The function of growth/differentiation factor 11 (Gdf11) in rostrocaudal patterning of the developing spinal cord

Jeh-Ping Liu

Hoxc family transcription factors are expressed in different domains along the rostrocaudal (RC) axis of the developing spinal cord and they define RC identities of spinal neurons. Our previous study using an in vitro assay system demonstrated that Fgf and Gdf11 signals located around Hensen's node of chick embryos have the ability to induce profiled Hoxc protein expression. To investigate the function of Gdf11 in RC patterning of the spinal cord in vivo, we expressed *Gdf11* in chick embryonic spinal cord by in ovo electroporation and found that ectopic expression of Gdf11 in the neural tissue causes a rostral displacement of Hoxc protein expression domains, accompanied by rostral shifts in the positions of motoneuron columns and pools. Moreover, ectopic expression of follistatin (Fst), an antagonist of Gdf11, has a converse effect and causes caudal displacement of Hox protein expression domains, as well as motoneuron columns and pools. Mouse mutants lacking Gdf11 function exhibit a similar caudal displacement of Hox expression domains, but the severity of phenotype increases towards the caudal end of the spinal cord, indicating that the function of Gdf11 is more important in the caudal spinal cord. We also provide evidence that Gdf11 induces Smad2 phosphorylation and activated Smad2 is able to induce caudal Hox gene expression. These results demonstrate that Gdf11 has an important function in determining Hox gene expression domains and RC identity in the caudal spinal cord.

KEY WORDS: Gdf11, Smad, Spinal cord, Hox, Rostrocaudal patterning

INTRODUCTION

The formation of a functional neuronal network requires the generation of distinct types of neurons at specific locations in the nervous system and, therefore, understanding how a progenitor cell acquires its specific fate is a fundamental issue of neurodevelopment. During development, signals originating from adjacent tissues pattern the neural plate along two major axes – dorsoventral (DV) and rostrocaudal (RC). Bone morphogenetic proteins (BMPs) originating from ectoderm and sonic hedgehog (Shh) protein originating from notochord are the major signals acting along the DV axis (for reviews, see Briscoe and Ericson, 2001; Helms and Johnson, 2003; Jessell, 2000), while retinoic acid (RA) originating from the somites, and fibroblast growth factors (Fgfs) and Wnt proteins originating from the regressing primitive streak/Hensen's node region are the major rostralizing and caudalizing signals acting along the RC axis (for a review, see Diez del Corral and Storey, 2004). Incorporation of the DV and the RC signals will then induce the expression of different transcription factors in neural progenitor cells located at different positions of the spinal cord, and these transcription factors in turn, determine neuronal identity.

Motoneurons are generated in the ventral spinal cord in response to Shh signaling (for reviews, see Briscoe and Ericson, 2001; Jessell, 2000), and their cell bodies segregate into different columns and pools at different RC positions according to their targets of innervation (Hollyday, 1980a; Hollyday, 1980b; Landmesser, 1978a; Landmesser, 1978b). Thus, lateral motor column (LMC) motoneurons that innervate limb musculature are present only at cervical/brachial and lumbar levels, while various motoneuron pools that innervate individual muscles are located at different RC positions. Hox family transcription factors are expressed in different RC domains in the spinal cord and they control the generation of specific motoneuron subtypes at each RC level (for reviews, see Carpenter, 2002; Krumlauf et al., 1993). Thus, Hoxc6, Hoxc9 and Hoxa10/Hoxd10 define motoneuron columnar identities at the brachial, thoracic and lumbar levels, respectively (Carpenter et al., 1997; Dasen et al., 2003; Lin and Carpenter, 2003; Shah et al., 2004), while Hoxc8 determines motor pool identities (Dasen et al., 2005; Vermot et al., 2005). Moreover, manipulating Hox gene expression also results in changes in spinal nerve projections (Burke and Tabin, 1996; Carpenter et al., 1997; Dasen et al., 2003; de la Cruz et al., 1999; Shah et al., 2004; Tiret et al., 1998).

Spinal cord stem cells are located around Hensen's node in chick, and the node in mouse embryos (Mathis and Nicolas, 2000; Schoenwolf, 1992). Progenitor cells designated for rostral spinal cord leave the stem zone prior to the progenitor cells designated for caudal spinal cord. Although the RC identities of these progenitor cells are specified when they leave the stem zone, their identity is still modifiable to a certain degree prior to somite formation (Ensini et al., 1998; Lance-Jones et al., 2001; Liu et al., 2001). In addition to the signaling factors, including Fgfs, Wnts and RA, that have been shown to control Hox gene expression in neural tissues (Bel-Vialar et al., 2002; Dupe et al., 1997; Marshall et al., 1994; Shimizu et al., 2005; Zhang et al., 1997), we have identified an additional activator of Hox gene expression, growth/differentiation factor 11 (Gdf11), using an in vitro assay system (Liu et al., 2001). Gdf11 is a transforming growth factor-β (TGF-β) family member and its expression begins at HH stage 10 (Hamburger and Hamilton, 1951) in chick embryos around Henson's node, caudal paraxial mesoderm and caudal neural plate (Liu et al., 2001). Similarly, *Gdf11* expression begins in the tail bud and caudal neural plate region in mouse embryos around E8.5 (Nakashima et al., 1999). Mouse mutants lacking Gdf11 die shortly after birth and exhibit six extra thoracic vertebrae, caudally displaced lumbar vertebrae and truncated tails (McPherron et al., 1999). A caudal displacement of Hox gene expression domains associated with the vertebral phenotype was observed in *Gdf11*$^{-/-}$ embryos, suggesting that Gdf11 has a role in patterning caudal structures (McPherron et al., 1999).

Department of Neuroscience, University of Virginia, 409 Lane Road, MR4, Room 5032, Charlottesville, VA 22908, USA.

e-mail: jl7nf@virginia.edu

Accepted 1 June 2006

In the olfactory epithelium, Gdf11 controls the number of olfactory receptor neurons by inhibiting the proliferation of their progenitors (Wu et al., 2003). However, in the developing retina, Gdf11 controls the number of retinal ganglionic cells by affecting the competence of progenitor cells but not their proliferation (Kim et al., 2005), indicating Gdf11 has a function in cell fate specification in addition to cell proliferation.

In this study, we investigate the function of Gdf11 in patterning spinal tissue in vivo. We manipulated Gdf11 levels in the developing spinal cord by expressing either *Gdf11* or its antagonist follistatin (*Fst*) (Gamer et al., 2001), using in ovo electroporation in early chick embryos. Our data demonstrate that Gdf11 has the ability to caudalize neural tissues by inducing caudal Hox gene expression and suppressing rostral Hox gene expression. This results in rostral displacements of Hox expression domains followed by changes in motoneuron identity and peripheral projection. These observations are further corroborated by analyses of the spinal cord phenotype in *Gdf11* loss-of-function mouse embryos – without endogenous Gdf11, these embryos exhibit caudal displacement and expansion of Hox expression domains, as well as a caudal shift in motoneuron columnar and pool positions. The severity of this phenotype increases towards the caudal end of the spinal cord, suggesting that Gdf11 function is more important for caudal neural identity. We also provide evidence that Gdf11 induces phosphorylation of Smad2 and activated Smad2 is able to control Hox gene expression. These data demonstrate that Gdf11 signaling through Smad2 plays a crucial role in determining Hox gene expression domains and neuronal identity in the caudal spinal cord.

MATERIALS AND METHODS

Expression constructs

To limit gene expression in neural progenitor cells, an expression vector (pNes-IRES-eGFP) was constructed by inserting a fragment from pHB9-GFP (Wichterle et al., 2002) containing a splicing substrate, multiple cloning sites and an IRES-eGFP cassette into the pNES1689tk vector (Zimmerman et al., 1994) containing the human nestin intron 2 enhancer followed by the HSV thymidine kinase promoter. Coding regions of the following genes were cloned into the pNES-IRES-GFP vector: human *Gdf11* (provided by S.-J. Lee), human follistatin (provided by M. Matzuk) and a constitutively activated Smad2-*Smad2E* (provided by M. Funaba).

In ovo electroporation

Electroporation was performed as described (William et al., 2003). Observation under a fluorescence microscope (Nikon SMZ1500) was made the day after electroporation and only embryos with visible GFP expression were used for analysis. Stages of embryos used for electroporation and the time of harvesting are indicated in the 'results' section. The *Gdf11* construct was used at 2-5 mg/ml; *Fst* and *Smad2-2E* constructs were used at 1-5 mg/ml.

Immunohistochemistry and in situ hybridization

For immunohistochemistry, mouse embryos were harvested at E12.5, and chick embryos were harvested 3 days after electroporation (~HH stage 25). Fixation, tissue preparation and antibody staining were performed as described (Liu and Jessell, 1998; Liu et al., 2001), and images were collected using a Nikon C-1 confocal microscope.

For in situ hybridization, chick embryos were harvested at various stages after electroporation, and mouse embryos were harvested at E12.5-E13.5. Whole-mount in situ hybridization was performed as described for chick (Thery et al., 1995), and for mouse embryos (Garces et al., 2000). A BCIP/NBT kit (Vector Labs) was used for the color reaction. Chick *Hoxc6-Hoxc10* probes were provided by C. Tabin. Mouse and chick *Raldh2*, *Pea3* and *Er81* probes, as well as mouse *Hoxc6* and *Hoxc10* probes were provided by T. Jessell and J. Dasen. All protocols for animal use were approved by the Institutional Animal Care and Use Committee of the University of Virginia and were in accordance with NIH guidelines.

For neurofilament staining, chick embryos were harvested 4-5 days after electroporation (HH stage 27-29), fixed overnight in 4% paraformaldehyde in 0.1 M phosphate buffer pH 7.4 at 4°C, then washed three times with PBS (1 hour/wash) before incubating with 0.15% H_2O_2 in PBS at 4°C overnight. Afterwards, the embryos were washed in PBS, and blocked in a solution of 10% heat-inactivated goat serum, 0.1% Triton X-100 in PBS (blocking buffer) for 6 hours. Embryos were then incubated with 3A10 antibody (DSHB) (1:150 dilution in blocking buffer) at 4°C overnight. Six 1-hour washes followed by a 3-hour blocking was performed the next day prior to the incubation with HRP-conjugated goat anti-mouse secondary antibody (Jackson Immuno) at 4°C overnight. The following day, six 1-hour washes with PBS were performed prior to detecting the signals using a VIP kit (Vector Labs).

Western analyses

Ventral neural plate explants were harvested from somite 5-8 chick embryos, prior to the onset of endogenous *Gdf11* expression, as described (Liu et al., 2001). Recombinant Gdf11 (R&D Systems) was added at various concentrations to F12 culture media supplemented with 2 mM glucose, N2 supplement, L-glutamine and penicillin/streptomycin (Invitrogen). After culturing for 1 hour at 37°C, total protein was extracted using extraction buffer [50 mM Tris pH 7.5, 400 mM NaCl, 1%NP40, 0.5% sodium deoxycholate, 0.1% SDS, 1 mM EDTA, 5 mM NaF, and protease inhibitors (Roche)]. Protein from 11 explants was used for each sample analysis.

Gdf11 electroporated embryos were harvested the day after electroporation (HH stage 14-15) and a 10-12 somite-long segment with high levels of GFP expression was isolated from each embryo. Each segment was separated in the midline and protein was extracted from both the electroporated and control sides for western analysis. Total protein from individual E9.5 mouse embryo was extracted and one-half of the protein from each embryo was used for western analysis. At least two sets of samples were collected for each experiment.

Phospho-Smad2/3, phospho-Smad1/5/8, Smad1 (for chick), Samd2 and Smad5 (for mouse) antibodies (Cell Signaling Technology) were used at 1:1,000 dilutions. SuperSignal West Femto Maximun sensitivity substrate (Pierce) was used as directed. Each blot was probed, stripped with Restore western blot stripping buffer (Pierce) and reprobed with a different antibody in the following order: pSmad1/5/8, Smad1 (chick) or Smad5 (mouse), pSmad2 and Smad2. Quantification of signals was performed using NIH ImageJ software (Abramoff, 2004).

RESULTS

Expression of *Gdf11* causes rostral displacement of Hox expression domains

To evaluate the function of Gdf11 in RC patterning of the neural tube, we first examined its expression pattern at different stages of development. The expression of *Gdf11* starts after the 10-somite stage in chick embryos, at the caudal end of the embryos, including the Henson's node, caudal paraxial mesoderm and neural plate (Liu et al., 2001). The rostral expression boundary of this caudal expression domain recedes as the embryos ages and by HH stages 21, the expression is confined to the tip of the tail bud (see Fig. S1A-D in the supplementary material). Around HH stage 15, *Gdf11* begins to express in the rostral spinal cord, coincident with the commencement of neurogenesis. The boundary of this expression domain extends caudally as the embryo ages and reaches the hindlimb level ~HH stage 21 (see Fig. S1A-D in the supplementary material). By this stage, Gdf11 is expressed highly in the differentiated neurons located at lateral positions in the spinal cord (see Fig. S1D in the supplementary material).

To examine the effect of Gdf11 on RC patterning of the neural tube, we expressed a cDNA encoding the human Gdf11 protein in somite 10-14 (HH stage 10-11) chick embryos using in ovo

electroporation. To confine gene expression to neural progenitor cells, when their RC identity is being defined, we constructed an expression vector (pNES-IRES-eGFP) controlled by a human nestin intron 2 enhancer (Zimmerman et al., 1994). An internal ribosomal reentry sequence (IRES) followed by an eGFP-coding region was placed into the same transcription unit to identify the cells that express the electroporated DNA. Using this construct, GFP expression can be detected ~4-6 hours after electroporation.

We first examined the effect of Gdf11 on Hoxc protein expression in HH stage 25 embryos 3 days after electroporation (Fig. 1A-H). In longitudinally sectioned spinal cords, a one to two segment rostral displacement in the expression domains of Hoxc6-Hoxc10 was observed in the electroporated sides in all embryos with strong GFP expression, an indicator of high electroporation efficiency (Fig. 1A-D). The shifts in Hoxc protein expression domains are also apparent in cross-sectioned spinal cords (Fig. 1E-H). We noticed a reduction in size of the electroporated side in the cross-sectioned spinal cord (Fig. 1E-H), which could reflect an anti-proliferative function of Gdf11 that was observed previously in the olfactory epithelium (Wu et al., 2003). To examine whether only motoneurons are affected, we assessed LH2, Lim1/2 and Isl 1/2 expression in HH stage 25 embryos 3 days after electroporation (see Fig. S2A-C in the supplementary material). The numbers of LH2^{+}(dI1), dorsal Isl1^{+}(dI3) and Lim1^{+}(dI2, dI4, dI6) neurons, as well as motoneurons were reduced to a similar degree (~61%-67% of the controls) in the electroporated side when compared with the control side, indicating that Gdf11 electroporation has a similar effect on cell proliferation at different DV positions.

To avoid possible complications generated by the proliferation effect of Gdf11 on analyzing the RC patterning phenotype, we examined Hox gene expression by in situ hybridization in HH stage 14-17 embryos 1 day after *Gdf11* electroporation, when motoneuron differentiation has just begun. We observed no difference in either the length of the neural tube or the number and size of the somites between the electroporated side and the control side (Fig. 1J-M′). Cross-sections through neural tubes of these embryos showed little difference in size between the electroporated and the control sides (data not shown). Nevertheless, a rostral expansion of *Hoxc6-Hoxc10* expression domain is clearly visible in the electroporated side (Fig. 1J-M), indicating that in the spinal cord, the function of Gdf11 in patterning/cell fate determination is independent from its function in proliferation.

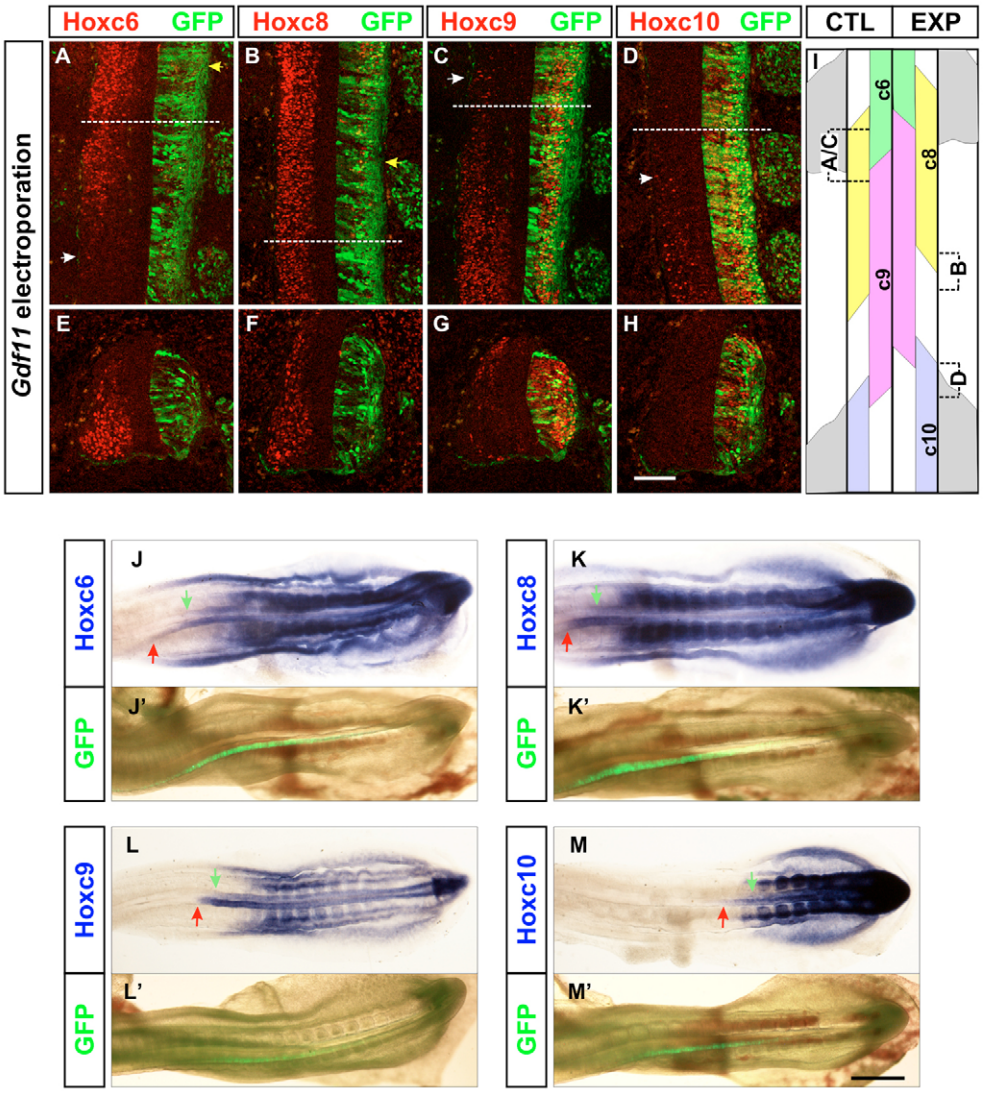

Fig. 1. Expression of *Gdf11* in the neural tube causes rostral displacement of Hox expression domains. (**A-H**) Hoxc6-Hoxc10 expression in longitudinally sectioned (A-D), and in cross-sectioned (E-H) spinal cords taken from HH stage 25 embryos 3 days after *Gdf11* electroporation. The electroporated side (on the right in all panels) is marked by GFP expression. White arrows indicate the caudal expression limit of Hoxc6 (A) and the rostral expression limits of Hoxc9 (C) and Hoxc10 (D) in the control side. Yellow arrows indicate the caudal expression limits of Hoxc6 (A) and Hoxc8 (B) in the electroporated side. (A,C) The same section double labeled with Hoxc6 and Hoxc9. Broken lines in A-D indicate the RC levels of sections (E-H). (E,G) The same section double labeled with Hoxc6 and Hoxc9; (F,H) the same section double labeled with Hoxc8 and Hoxc10. (**I**) A diagram depicts the normal Hox expression domains in the control (CTL) side and the rostral displacement of Hox expression domains in the *Gdf11* electroporated side (EXP) of the spinal cord. Brackets indicate the RC levels of A-D. Position of the limbs is represented by gray-colored areas. Scale bar: 100 μm. (**J-M**) Hoxc6-Hoxc10 expression and (J′-M′) GFP expression in HH stage 15-17 embryos 20-24 hours after *Gdf11* electroporation. The electroporated side is towards the bottom of the panels. Red and green arrows indicate the rostral limit of Hoxc6-Hoxc10 expression in the electroporated and the control side, respectively. Scale bar: 0.5 mm.

Expression of *Gdf11* causes rostral displacement of motoneuron column and pool markers and spinal nerve projections

The functions of Hoxc6 and Hoxc9 are important in defining brachial level and thoracic level motoneuron identity, respectively (Dasen et al., 2003). Therefore, we next examined if the changes in Hox expression domains induced by Gdf11 are followed by changes in motoneuron identity. Spinal cords from HH stage 29 embryos 5 days after *Gdf11* electroporation were isolated, and the expression pattern of a lateral motor column (LMC) marker, *Raldh2* (Sockanathan and Jessell, 1998), was examined by in situ hybridization (Fig. 2A). A rostral shift of *Raldh2* expression domains was observed at both brachial and lumbar levels in the electroporated side (Fig. 2A), indicating that the rostrally displaced Hox expression domains are able to induce a corresponding shift in motoneuron columnar identity. Loss of Hoxc8 function in both chick and mouse embryos results in the loss of *Pea3* expression in motoneuron pools located in the brachial level spinal cord (Dasen et al., 2005; Vermot et al., 2005). Therefore, we also examined the expression of *Pea3* and another motor pool marker *Er81* (Lin et al., 1998) in spinal cords isolated from *Gdf11* electroporated embryos. Rostral displacements of *Pea3* and *Er81* expression domains were also observed in the electroporated side at both brachial and lumbar levels (Fig. 2B; data not shown).

To determine if the axons originating from the rostrally displaced LMC motoneurons are able to project to appropriate targets, we used an antibody against neurofilament (3A10) to visualize spinal nerve projections in HH stage 29 embryos 5 days after *Gdf11* electroporation. In the control side of the embryos, spinal nerves 13-16 and a small region of spinal nerve 17 innervate the forelimb (Hollyday and Jacobson, 1990). However, a ~one-segment rostral shift in the spinal nerves that project to the forelimb was observed in the electroporated side (Fig. 2C). At the hindlimb level, spinal nerves that innervate the crural plexus originate normally from lumbosacral (LS) level 1-3, and to a lesser extent from thoracic (T) level 7 (Lance-Jones and Dias, 1991), as seen in the control side (Fig. 2D). An approximately one-segment rostral shift in spinal nerves that innervate the crural plexus and the spinal nerves that innervate the thoracic region was observed in the electroporated side (Fig. 2C,D). The extent of the rostral shift of the spinal nerve projections depends upon the efficiency of electroporation – in most cases an approximately one-segment rostral shift was observed in embryos harvested at HH stage 29. Surprisingly, a rostral shift in limb positions at the electroporated side was also observed in ~85% (24/28) of the *Gdf11* electroporated embryos. The shift is more apparent at the hindlimb level (Fig. 2D) but can also occur in the forelimbs (data not shown). Depending upon the extent of *Gdf11* expression, independent forelimb or hindlimb shift was also detected.

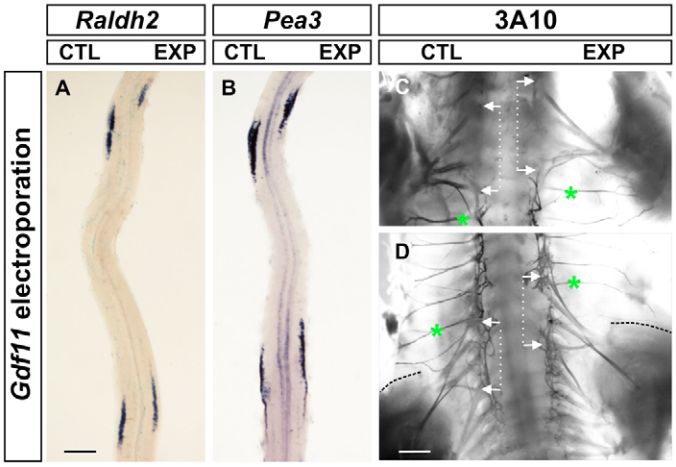

Fig. 2. Expression of *Gdf11* in the neural tube results in rostral displacement of motor neuron column and pool positions. (**A**) *Raldh2* and (**B**) *Pea3* expression in the spinal cord and (**C**,**D**) neurofilament (3A10) staining in HH stage 29 embryos 5 days after *Gdf11*electroporation. The electroporated side (EXP) is on the right of all panels, while the control side (CTL) is on the left. Rostral is towards the top and caudal is towards the bottom. White brackets indicate the origins of the spinal nerves that innervate the forelimbs in C and the hindlimbs in D. Green asterisks mark the first (C) and the last (D) spinal nerves that innervate the thoracic levels. Broken black lines mark the rostral boundaries of the hindlimbs in D. Scale bars: 0.5 mm.

These results demonstrate that elevated levels of Gdf11 are able to induce rostral displacement in Hox gene expression domains, accompanied by rostral shift in motor neuron columns and pools, thus caudalizing the neural tube in the electroporated side.

Expression of follistatin causes caudal displacement of Hox expression domains and motoneuron identity in the spinal cord

If increased levels of Gdf11 are able to caudalize the spinal cord, we reasoned that reducing the level of Gdf11 should have the opposite effect. Therefore, we expressed an antagonist of Gdf11 – follistatin (Fst) (Gamer et al., 2001) in neural progenitor cells to suppress the function of endogenous Gdf11. A cDNA encoding human Fst was cloned into the pNes-IRES-eGFP expression vector and electroporated into somite 10-17 chick embryos. Immunohistochemical analyses for Hoxc protein expression were performed on HH stage 25 embryos 3 days after electroporation. In contrast to the rostral shift of Hoxc expression domains observed in *Gdf11* electroporated embryos, a one to two segment caudal displacement in the expression domains of Hoxc6-Hoxc10 was observed in the *Fst* electroporated side (Fig. 3A-H), indicating that appropriate levels of Gdf11 signaling are required in the neural tube to define proper Hox expression domains.

As Fst is also an antagonist to BMP family proteins that pattern dorsal spinal cord, we therefore examined LH2, Lim1/2, and Isl 1/2 expression in cross-sectioned spinal cords of HH stage 25 embryos 3 days after electroporation (see Fig. S2D-F in the supplementary material). There is no significant change in the number of motoneurons, but a ~35% reduction of $LH2^+$ neurons, a ~45% reduction of dorsal Isl^+ neurons, and a ~27% reduction of $Lim1^+$ neurons was detected in the electroporated side (see Fig. S2D-F in the supplementary material; data not shown).

Associated with the displaced Hox expression domains, *Raldh2*, *Pea3* and *Er81* expression in spinal cords isolated from embryos 5 days after *Fst* electroporation also exhibit a corresponding caudal shift in the electroporated side (Fig. 4A,B; data not shown). Examination of spinal nerve projections in embryos electroporated with *Fst* revealed an approximately one-segment caudal shift of the spinal nerves projecting into the forelimbs, the hindlimbs and the intervening thoracic regions in the electroporated side (Fig. 4C,D). In addition, a caudal shift of limb positions (either the forelimb, the hindlimb or both) was observed in ~70% of the electroporated embryos (20/28) (Fig. 4D).

These results suggest that the amount of Gdf11 a neural progenitor receives helps to determine the RC identity of its neuronal descendents. A higher concentration of Gdf11 at a given RC position

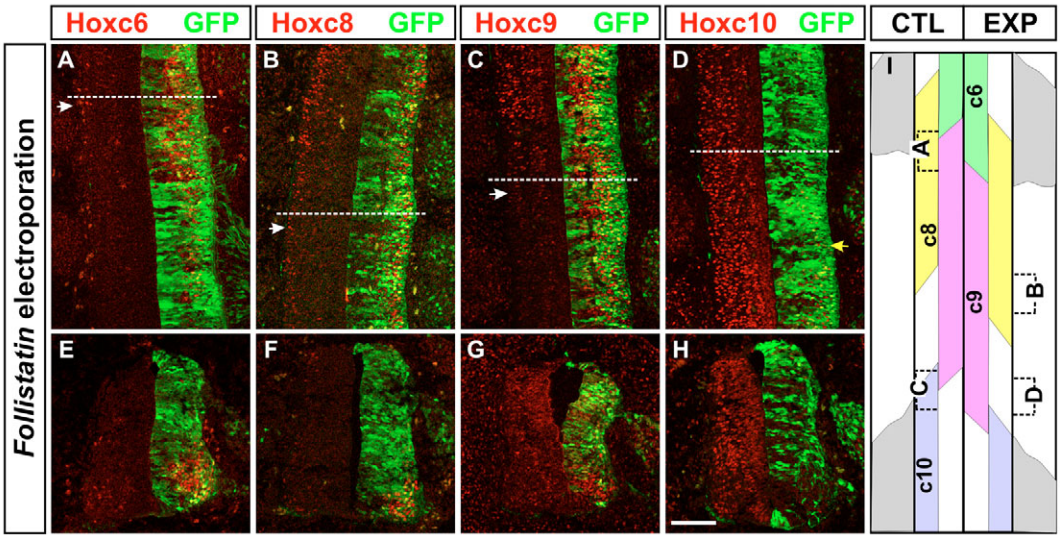

Fig. 3. Expression of follistatin (*Fst*) in the neural tube causes caudal displacement of Hox protein expression domains. (**A-H**) Hoxc6-Hoxc10 expression in longitudinally sectioned (A-D), and in cross-sectioned (E-H) spinal cords taken from HH stage 25 embryos 3 days after *Fst* electroporation. The electroporated side (on the right in all panels) is marked by GFP expression. White arrows indicate the caudal expression limits of Hoxc6 (A), Hoxc8 (B) and Hoxc9 (C) in the control sides. Yellow arrow indicates the rostral expression limit of Hoxc10 (D) in the electroporated side. Broken lines in A-D indicate the RC levels of sections (E-H). (**I**) A diagram depicts the normal Hox expression domains in the control (CTL) side and the caudal displacement of Hox expression domains in the *Fst* electroporated side (EXP) of the spinal cord. Brackets indicate the RC levels of A-D. Position of the limbs is represented by gray-colored areas. Scale bar: 100 μm.

will drive the progenitor cell towards a more caudal identity, while a lower concentration of Gdf11 ensures a more rostral identity. The RC identity change in the progenitor cells is reflected by changes in Hox gene expression domains, and results in the generation of motoneuron columns and pools at new positions along the RC axis.

Mouse mutants lacking Gdf11 function exhibit rostralized neural identity

The results of manipulating Gdf11 levels in chick neural progenitor cells suggest a function for Gdf11 in the overall RC patterning of the spinal cord. However, the onset of *Gdf11* expression in chick embryos begins around HH stage 10, a time when most progenitor cells designated for cervical levels have already left the stem zone, indicating that the endogenous function of Gdf11 might be limited to patterning the caudal spinal cord. To examine the normal function of Gdf11 in RC patterning of neural tissues, we used a strain of Gdf11 loss-of-function mice (McPherron et al., 1999).

Hoxc6-Hoxc10 gene expression in spinal cords isolated from E12.5 *Gdf11*$^{-/-}$ embryos and their control littermates was examined by whole-mount in situ hybridization (Fig. 5A-D and data not shown). The overall length of the spinal cord is very similar between mutants and their control littermates at this stage (Fig. 5A-D), albeit the truncated tails are clearly visible in the mutants (data not shown). The position of the rostral *Hoxc8* expression boundary is very similar between the mutants and controls, but the caudal boundary extends more caudally in the mutants (Fig. 5A,B). By contrast, the entire expression domain of *Hoxc10* is shifted caudally in the *Gdf11* mutants (Fig. 5C,D).

To examine the changes in Hox expression in more detail, we performed immunohistochemical analyses of Hoxc5-Hoxc10 protein expression in spinal cords isolated from E12.5 *Gdf11*$^{-/-}$ and control littermates at different RC levels (Fig. 6A-J and data not shown). We did not detect a significant difference in the Hoxc5 expression domain, nor in the rostral expression boundaries of Hoxc6 and Hoxc8 between *Gdf11*$^{-/-}$ and control embryos (data not shown). However, the caudal boundary of Hoxc6 expression shifted approximately one segment caudally (Fig. 6A,B), while the caudal boundary of Hoxc8 expression domain shifted approximately five segments caudally (Fig. 6C,D) in the *Gdf11*$^{-/-}$ spinal cords when compared with the controls. The rostral and caudal expression boundaries of Hoxc9 exhibit an approximately one-segment and a six-segment caudal shift, respectively (Fig. 6E,F and data not shown), while the entire expression domain of Hoxc10 shifted approximately six segments caudally (Fig. 6G-J).

These results demonstrate that Hox expression patterns at the cervical level are essentially normal in *Gdf11*$^{-/-}$ embryos. However, a caudal expansion of Hoxc6-Hoxc10 expression was observed starting from the thoracic level, and the degree of expansion increases progressively towards the caudal end of the neural tube. This results in an approximately one-segment expansion of the cervical level spinal cord, an approximately one-segment caudal displacement and approximately five-segment expansion of the thoracic level spinal cord, and a approximately six segment caudal displacement and elongation of the lumbar level spinal cord at the expense of the sacral spinal cord.

Along with the caudal expansion of Hoxc expression domains in the *Gdf11*$^{-/-}$ spinal cord, changes in the expression domains of the LMC marker *Raldh2* and motoneuron pool marker *Pea3* are also observed (Fig. 5E-H). Whole-mount in situ hybridization performed on isolated E13.5 spinal cords revealed that the rostral boundaries of cervical LMC and *Pea3*+ motoneuron pools are maintained at similar RC positions in the control and the mutant embryos. However, the caudal boundaries of cervical LMC and *Pea3* expression domain extend more caudally in the *Gdf11*$^{-/-}$ spinal cord when compared with that of the controls (Fig. 5E-H). By contrast, not only the entire *Raldh2* and *Pea3* expression domains at the lumbar level shift caudally but the length of these domains are also increased in the *Gdf11*$^{-/-}$ spinal cords (Fig. 5E-H).

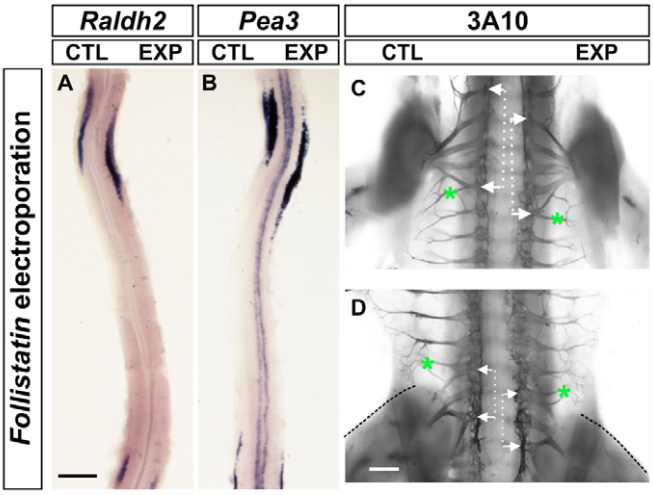

Fig. 4. Expression of *Fst* in the neural tube results in caudal displacement of motor neuron column and pool positions. (**A**) *Raldh2* and (**B**) *Pea3* expression in HH stage 29 spinal cords 5 days after *Fst* electroporation. (**C**,**D**) Neurofilament (3A10) staining of HH stage 27 embryos 4 days after *Fst* electroporation. The electroporated side (EXP) is on the right of all panels while the control side (CTL) is on the left. Rostral is towards the top and caudal is towards the bottom. White brackets mark the origins of the spinal nerves that innervate the forelimbs in C and the hindlimbs in D. Green asterisks mark the first (C) and the last (D) spinal nerves that innervate the thoracic levels. Broken black lines mark the rostral boundaries of the hindlimbs in D. Scale bars: 0.5 mm.

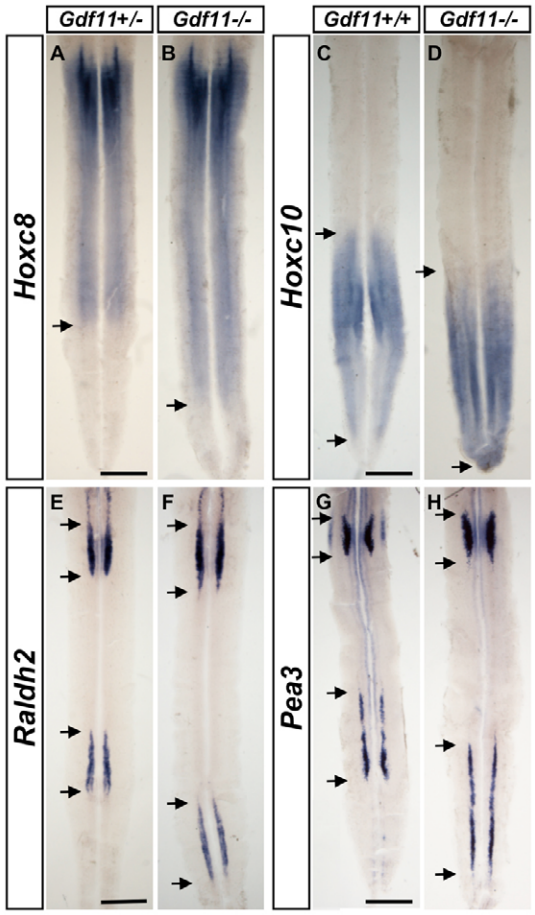

Fig. 5. Caudal displacement of Hox expression domains, motoneuron column and pool positions in *Gdf11*$^{-/-}$ spinal cord. (**A-D**) *Hoxc8* and *Hoxc10* expression in flat-mounted open-book preparations of spinal cords isolated from E12.5 control (A,C) and *Gdf11*$^{-/-}$ (B,D) mouse embryos. Rostral is towards the top and caudal is towards the bottom. The caudal boundary of *Hoxc8* expression is indicated by arrows in A,B, while the *Hoxc10* expression domain is located between arrows in C,D. (**E-H**) *Raldh2* and *Pea3* expression in flat-mounted open-book preparations of spinal cords isolated from E13.5 control (E,G) and *Gdf11*$^{-/-}$ (F,H) mouse embryos. Rostral is towards the top and caudal is towards the bottom. Arrows indicate the expression boundaries of *Raldh2* and *Pea3*. Scale bars: 1 mm.

These results demonstrate that Gdf11 plays a role in assigning RC identity to the spinal cord in both chick and mouse embryos. However, endogenous Gdf11 function is most probably required for patterning the caudal spinal cord from thoracic to sacral levels, as the RC identity of the cervical spinal cord is essentially normal in *Gdf11*$^{-/-}$ embryos, while the severity of the rostralization phenotype increases towards the caudal end of the spinal cord.

Gdf11 induces caudal Hox gene expression through activation of Smad2

How does Gdf11 exert its function in inducing caudal Hox gene expression? TGFβ family proteins bind to hetromeric type II and type I receptors, induce phosphorylation of Smad proteins, and affect gene transcription (for reviews, see Massague et al., 2005; Shi and Massague, 2003). Activin type II receptor 2A and 2B were shown to mediate the function of Gdf11 in axial patterning in mouse, and Gdf11 was shown to induce the phosphorylation of Smad2 and reduce the level of phospho-Smad1 in *Xenopus* ectodermal explants (Oh et al., 2002). We therefore, examined if Smad proteins are involved in mediating the function of Gdf11 in inducing caudal Hox gene expression.

We first harvested ventral neural plate from five- to eight-somite chick embryos (Liu et al., 2001), prior to the expression of endogenous Gdf11, and cultured them in serum-free medium for 1 hour with or without Gdf11. Total protein extracted from these explants was then used in western analyses to detect phospho-Smad 1/5/8 (p-Smad1/5/8) and phospho-Smad 2/3 (p-Smad2/3) levels (Fig. 7A). A concentration-dependent induction of p-Smad2/3 was observed with the addition of Gdf11: a ~60-fold induction by 10 ng/ml Gdf11; a ~100-fold induction by 25 ng/ml Gdf11; and a ~230-fold induction by 50 ng/ml Gdf11 (Fig. 7A; data not shown). By contrast, p-Smad1/5/8 was reduced to ~20% of the control when treated with 10ng/ml Gdf11 (Fig. 7A), and to ~50% of the control with 25 ng/ml Gdf11 (data not shown), while 50 ng/ml Gdf11 increases p-Smad1/5/8 levels approximately threefold over the control (Fig. 7A). These results demonstrate that in vitro, Gdf11 activates the phosphorylation of Smad2/3 very efficiently, but, by contrast, it inhibits the phosphorylation of Smad1/5/8 at lower concentrations while inducing their phosphorylation at higher concentrations.

To verify if the same effects are present in vivo, we electroporated somite 11-12 chick embryos with *Gdf11* and harvested the embryos 1 day later around HH stage 14-15. A segment of each embryo with high GFP expression was isolated and the control and electroporated sides were separated along the midline and used for western analysis (see Fig. S3A in the supplementary material). An approximately

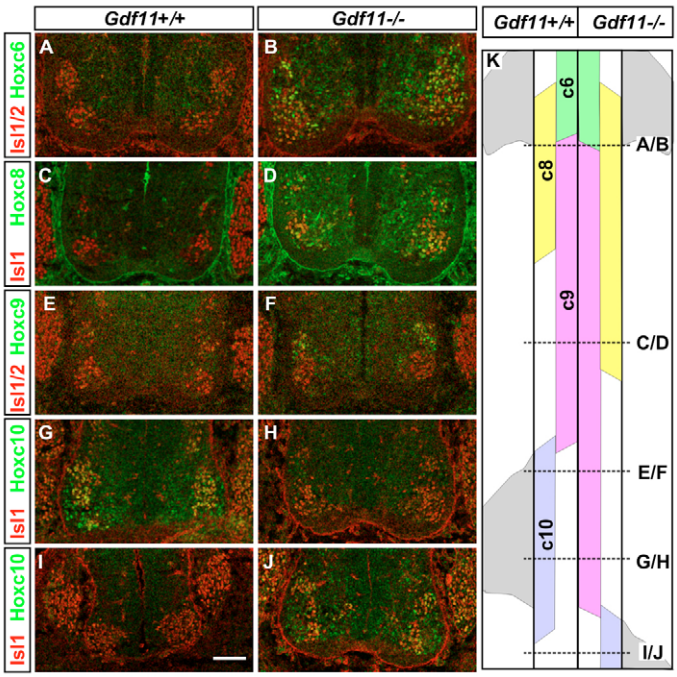

Fig. 6. Caudal displacement and expansion of Hox protein expression domains in *Gdf11*$^{-/-}$ mouse embryos. (**A-J**) Hoxc6-Hoxc10 expression in cross-sectioned E12.5 ventral spinal cords isolated from *Gdf11*$^{+/+}$ (A,C,E,G,I) and *Gdf11*$^{-/-}$ (B,D,F,H,J) mouse embryos. Motoneurons and dorsal root ganglia are marked by Isl1 or Isl1/2 expression. (**K**) A diagram depicts the Hox expression domains in *Gdf*$^{+/+}$ and *Gdf*$^{-/-}$ spinal cords. Broken lines indicate the RC levels in A-J. Position of the limbs is represented in gray. Scale bar: 100 μm.

twofold increase in p-Smad2/3 was observed in the electroporated side when compared with the control side, while no significant change of p-Smad 1/5/8 was detected (Fig. 7B). Similarly, a ~50% reduction in p-Smad2/3 but no apparent change in p-Smad1/5/8 level was detected in *Gdf11*$^{-/-}$ embryos when compared with their wild-type littermates at E9.5 (Fig. 7C), a stage when *Gdf11* is only expressed in the caudal region (see Fig. S3B in the supplementary material).

To examine the function of Smad2 in controlling Hox gene expression more directly, we obtained a constitutively activated form of Smad2, Smad2-2E, that contains Ser→Glu changes at amino acid 465 and 467 of the Smad2 protein (Funaba and Mathews, 2000). A construct expressing *Smad2-2E* was electroporated into somite 9-14 chick embryos, and Hoxc6-Hoxc10 protein expression was analyzed 3 days later at HH stage 24-25. As Smad2 is a transcription factor, we did not anticipate significant Hox expression domain shifts as observed in the *Gdf11* and *Fst* electroporated embryos. Nevertheless, a caudalizing effect on Hox protein expression was observed in cells with strong GFP expression (indicating high levels of Smad2-2E expression) (Fig. 7D-M). Hoxc9 and Hoxc10 induction is clearly visible in cells expressing high levels of Smad2-2E (Fig. 7F,G,K,L), while Hoxc6 and Hoxc8 expression was simultaneously suppressed (Fig. 7D,E,I,J). Smad2-2E induced Hoxc9-expressing cells never co-express Hoxc6, although they are located in the Hoxc6 expression domain (Fig. 7H,M), as observed in Fgf-induced Hoxc9 expression (Dasen et al., 2003). This result demonstrates that Gdf11 can affect Hox gene expression through a Smad2-mediated pathway.

DISCUSSION

Gdf11 functions in rostrocaudal patterning of the spinal cord in vivo

Using both chick and mouse embryos, we demonstrate that the level of Gdf11can affect the RC identify of the spinal cord by changing the Hox expression profile, and subsequent neuronal identity change will follow according to the changed Hox code. Thus, motoneuron columns and pools will develop at new RC positions where appropriate combinations of Hox codes are present. These motoneurons extend axons to their peripheral targets, according to their new RC identity and, therefore, a shift in the spinal nerve positions was also detected. This in vivo effect of Gdf11 on the RC patterning of the spinal cord is most probably superimposed upon pre-existing Fgf signals based on the following reasons: first, Fgf signals have been shown to induce neural Hox gene expression (Bel-Vialar et al., 2002; Dasen et al., 2003; Liu et al., 2001); and second, although a rostralization phenotype was observed in the *Gdf11*$^{-/-}$ embryos, a rostral to caudal difference still exists suggesting that even without Gdf11, Fgf signals are able to pattern the spinal cord to a certain degree.

Spinal cord stem cells are located around Hensen's node in chick, and the node in mouse embryos (Mathis and Nicolas, 2000; Schoenwolf, 1992), where high concentrations of Fgf are present. The function of Fgf is important in initiating and maintaining the stem zone identity and in inducing caudal neural properties (Delfino-Machin et al., 2005; Diez del Corral et al., 2003; Mathis et al., 2001). The expression of *Gdf11* begins at HH stage 10 in and around Hensen's node where high levels of Fgf signals are present. At this stage, most of the progenitor cells designated for cervical/brachial levels have already left the stem zone. Therefore, the combined activities of Fgf and Gdf11 will most probably determine the expression patterns of Hox genes and the RC identity of caudal spinal neurons (Fig. 8A).

The RC identities of the spinal progenitor cells are specified when they leave the stem zone; however, their identity is still modifiable to a certain degree prior to somite formation (Ensini et al., 1998; Lance-Jones et al., 2001; Liu et al., 2001). Therefore, the function of Gdf11 in controlling RC identity is most probably exerted upon the progenitor cells prior to somite formation and neurogenesis. When *Gdf11* is expressed in the neural tube by in ovo electroporation, progenitor cells are exposed to ectopic Gdf11 in addition to pre-existing Fgf/Gdf11 signals, resulting in a rostral displacement of the Hox expression domains, as well as motoneuron columns and pools (Fig. 8B). By contrast, when *Fst* is expressed in the neural tube, a fraction of endogenous Gdf11 signaling is inhibited, leading to caudal displacement of Hox expression domains and motoneuron columns and pools.

In a mouse mutant lacking Gdf11, Fgf signals are able to pattern the neural tube to a certain degree with a slight caudal expansion of cervical identity, in contrast to the significant caudal displacement and expansion of thoracic and lumbar identities. We do not have spinal cord markers that are expressed in a more caudal position than *Hoxc10*; however, judging from the caudal extent of *Raldh2* and *Pea3* expression, the sacral region in these embryos is most probably transformed into lumbar identity (Fig. 8C). These results suggest that Gdf11 has a function in determining Hox gene expression and neuronal identity in the caudal spinal cord.

Both Fgfs and Gdf11 have functions in controlling Hox gene expression and our previous results have demonstrated that low concentrations of Fgf are required for Gdf11 to induce caudal Hox gene expression in vitro (Liu et al., 2001), suggesting Gdf11 could

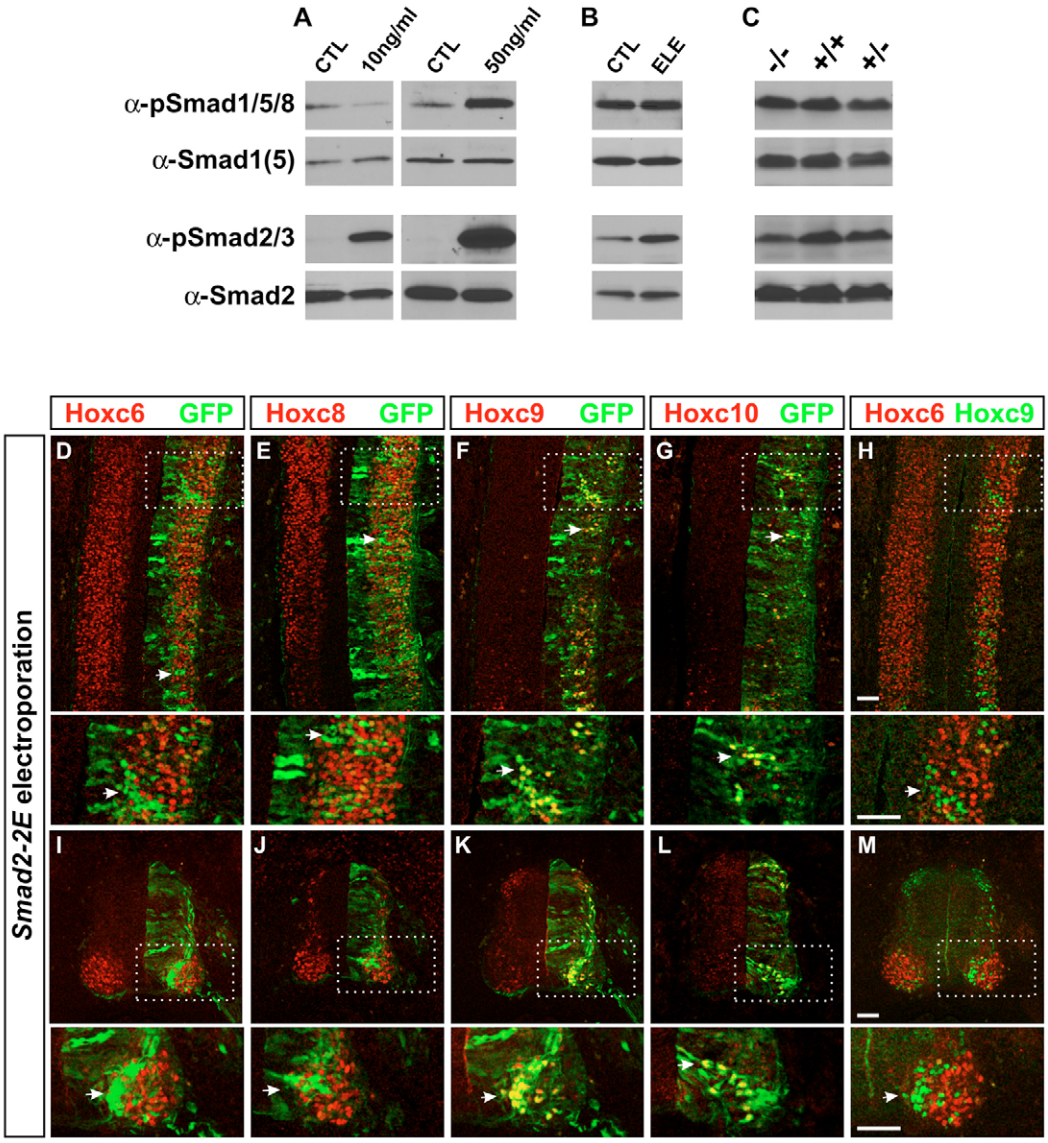

Fig. 7. Expression of a constitutively activated Smad2 (*Smad2-2E*) induces caudal Hox protein expression at the expense of rostral Hox protein expression. (**A-C**) Western analyses of pSmad1/5/8 and pSmad2/3 levels in neural plate explants treated with Gdf11 (A), in *Gdf11* electroporated chick embryos (B) and in E9.5 *Gdf11*$^{-/-}$ mouse embryos (C). (**D-M**) Hoxc6-Hoxc10 expression in longitudinally sectioned (D-H) and in cross-sectioned (I-M) HH stage 25 spinal cords 3 days after *Smad2-2E* electroporation. The electroporated side (on the right in all panels) is marked by GFP expression. Enlarged image of boxed areas are shown below each panel. White arrows indicate the inhibition of Hoxc6 (D,I) and Hoxc8 (E,J) expression, and the induction of Hoxc9 (F,K) and Hoxc10 (G,L) expression by *Smad2-2E* expression. Double labeling of Hoxc6 and Hoxc9 (H,M) demonstrate the Hoxc9^{+} cells (white arrows) induced by *Smad2-2E* in the Hoxc6 domain do not express Hoxc6. (D,F,H) The same section; (I,K,M) the same section. Scale bars: 50 μm.

increase response of the progenitor cells to Fgf signals. Further studies will be required to elucidate the level of interaction between the Fgf and Gdf11 signaling pathways and the molecules involved.

Smad2 mediates the function of Gdf11 in controlling Hox expression

Our data demonstrate that the induction of p-Smad2/3 level by Gdf11 is very efficient in vitro. However, the changes in p-Smad2/3 levels that were induced by *Gdf11* electroporation or reduced in *Gdf11*$^{-/-}$ embryos are not as dramatic as that observed in vitro. Judging from the small percentage of cells (<10%) that actually express Gdf11 in the in vivo samples (see Fig. S3 in the supplementary material), a high local level of p-Smad2/3 in the vicinity of Gdf11-expressing cells would be under-represented when the whole tissue is used in western analyses. No significant change in pSmad1/5/8 levels was observed in the in vivo samples, which could be due to a localized effect masked by analyzing the whole tissue as discussed above. Alternatively, the changes in pSmad1/5/8 levels observed in vitro could be an artifact caused by very high concentrations of the recombinant Gdf11. Nevertheless, without an antibody against pSmad1/5/8 that works reliably for immunohistochemical analysis, we are uncertain if the local Gdf11 concentration is high enough to induce the phosphorylation of Smad1/5/8 in vivo.

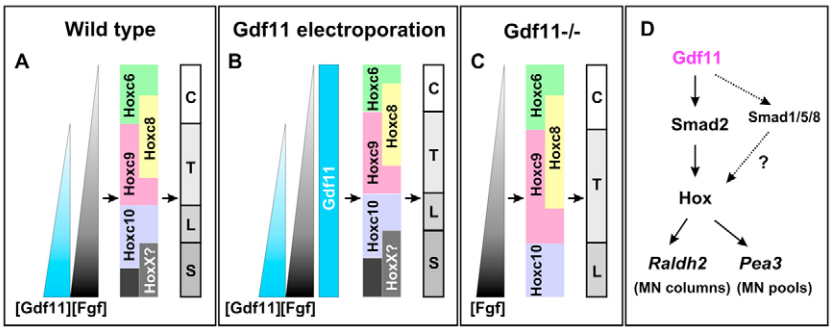

Fig. 8. A model for Gdf11 function in controlling Hox gene expression and rostrocaudal identity in the spinal cord. (**A**) Normally, the onset of *Gdf11* expression begins after most of the cervical progenitor cells leave the stem zone, and therefore, only progenitor cells designated for caudal levels receive the Gdf11 signal. Fgf and Gdf11 work together to define *Hox* gene expression domains in the caudal spinal cord. (**B**) *Gdf11* electroporation increases the level of Gdf11 and, thus, results in a rostral displacement of *Hoxc6-Hoxc10* domains. (**C**) In *Gdf11*$^{-/-}$ embryos, only the Fgf signal remains. This causes severe caudal displacement and expansion in *Hoxc10* and *Hoxc9* domains, respectively, and a lesser effect in *Hoxc6* and *Hoxc8* domains. (**D**) A model for Gdf11 function in the control of Hox gene expression and RC identity of the spinal cord. Smad2 mediates the function of Gdf11 in promoting caudal Hox gene expression. Although high levels of Gdf11 can activate the Smad1/5/8 pathway in vitro, the significance of this pathway in vivo requires further examination.

Misexpression of a constitutively activated form of Smad2 (Smad2-2E) in neural tissue is able to mimic the function of Gdf11 in inducing Hoxc9/Hoxc10 and inhibiting Hoxc6/Hoxc8 expression, demonstrating more directly that Smad2 mediates the function of Gdf11 in controlling Hox gene expression in vivo (Fig. 8D). Smad transcription factors could act directly on Hox genes to induce/repress their expression, and several potential Smad-binding elements (SBE, 5′-CAGAC-3′ or 5′-GTCT-3′) are present in the *Hoxc9-Hoxc8* intergenic region, as well as in the intron of *Hoxc8*. Alternatively, Smad2 could control Hox gene expression indirectly through the Cdx genes, which are key mediators involved in integrating Fgf, RA and Wnt signals in inducing Hox gene expression (for a review, see Lohnes, 2003).

Our current data cannot rule out the possibility that other molecules, including Smad1/5/8, are also involved in mediating the function of Gdf11. Moreover, one of the Gdf family member (Gdf7) is able to form heterodimers with BMPs (Butler and Dodd, 2003), and BMP1 can activate a latent form of Gdf11 (Ge et al., 2005), thus further increasing the complexity of the potential signaling pathways involved. Unfortunately, Smad1 loss-of-function mouse mutants die around E9.5 (Lechleider et al., 2001), while Smad2 mouse mutants die around gastrulation (Waldrip et al., 1998) before their function in RC patterning of the spinal cord can be assessed. Conditional mutants of these genes will help to confirm the participation of Smad proteins in mediating the function of Gdf11 function.

Limb position changes associated with changes in neural Gdf11 levels

We observed an unexpected rostral shift in limb positions in embryos electroporated with *Gdf11* and a caudal shift in limb positions in embryos electroporated with *Fst* using an enhancer that directs gene expression in neural progenitor cells. The observed limb position change may be induced by Gdf11 secreted from the neural tube, or by Gdf11 secreted from neural crest cells that have migrated into the somites in the electroporated side. Alternatively, an as yet unknown factor that is controlled by the neural Hox code and secreted by the neural tube could act as a feedback mechanism to ascertain that the limb positions are in register with the positions of the LMC motoneurons. Previous studies have demonstrated that axial and paraxial mesoderm influence rostrocaudal patterning of the neural tube (Ensini et al., 1998; Lance-Jones et al., 2001). However, there is no evidence so far for the existence of a feedback signal from the neural tissue to the adjacent mesoderm. Although *Gdf11*$^{-/-}$ embryos exhibit a caudal displacement in their hindlimb positions along with the caudal displacement of neuronal identity, Gdf11 may be functioning independently in both mesoderm and neural tissues in this case. Further studies are required to reveal the mechanism that underlie the shift of limb positions observed in these electroporated embryos.

We thank Drs S.-J. Lee, T. Jessell, J. Dasen, C. Tabin, M. Funaba, M. Matzuk and I. Lieberam for providing essential materials that were critical for this work; A. Burke, J. Dasen and T. Jessell for discussion; J. Dasen, T. Jessell, B. Winckler and S. Zeitlin for critical reading of the manuscript and comments. J. Blackburn, K. Bowman and K. Lwin made various expression constructs used in this study, and C. Cathcart advised in image acquisition. This study was supported by a NIH grant (R01 NS045933) and the Burroughs Wellcome Career Award in Biomedical Sciences to J.-P.L.

Supplementary material

Supplementary material for this article is available at
http://dev.biologists.org/cgi/content/full/133/15/2865/DC1

References

Abramoff, M. D., Magelhaes, P. J. and Ram, S. J. (2004). Image processing with ImageJ. *Biophotonics Int.* **11**, 36-42.
Bel-Vialar, S., Itasaki, N. and Krumlauf, R. (2002). Initiating Hox gene expression: in the early chick neural tube differential sensitivity to FGF and RA signaling subdivides the HoxB genes in two distinct groups. *Development* **129**, 5103-5115.
Briscoe, J. and Ericson, J. (2001). Specification of neuronal fates in the ventral neural tube. *Curr. Opin. Neurobiol.* **11**, 43-49.
Burke, A. C. and Tabin, C. J. (1996). Virally mediated misexpression of Hoxc-6 in the cervical mesoderm results in spinal nerve truncations. *Dev. Biol.* **178**, 192-197.
Butler, S. J. and Dodd, J. (2003). A role for BMP heterodimers in roof plate-mediated repulsion of commissural axons. *Neuron* **38**, 389-401.
Carpenter, E. M. (2002). Hox genes and spinal cord development. *Dev. Neurosci.* **24**, 24-34.
Carpenter, E. M., Goddard, J. M., Davis, A. P., Nguyen, T. P. and Capecchi, M. R. (1997). Targeted disruption of Hoxd-10 affects mouse hindlimb development. *Development* **124**, 4505-4514.
Dasen, J. S., Liu, J. P. and Jessell, T. M. (2003). Motor neuron columnar fate imposed by sequential phases of Hox-c activity. *Nature* **425**, 926-933.
Dasen, J. S., Tice, B. C., Brenner-Morton, S. and Jessell, T. M. (2005). A hox regulatory network establishes motor neuron pool identity and target-muscle connectivity. *Cell* **123**, 477-491.
de la Cruz, C. C., Der-Avakian, A., Spyropoulos, D. D., Tieu, D. D. and Carpenter, E. M. (1999). Targeted disruption of Hoxd9 and Hoxd10 alters locomotor behavior, vertebral identity, and peripheral nervous system development. *Dev. Biol.* **216**, 595-610.
Delfino-Machin, M., Lunn, J. S., Breitkreuz, D. N., Akai, J. and Storey, K. G. (2005). Specification and maintenance of the spinal cord stem zone. *Development* **132**, 4273-4283.
Diez del Corral, R. and Storey, K. G. (2004). Opposing FGF and retinoid pathways: a signalling switch that controls differentiation and patterning onset in the extending vertebrate body axis. *BioEssays* **26**, 857-869.
Diez del Corral, R., Olivera-Martinez, I., Goriely, A., Gale, E., Maden, M. and Storey, K. (2003). Opposing FGF and retinoid pathways control ventral neural

pattern, neuronal differentiation, and segmentation during body axis extension. *Neuron* **40**, 65-79.
Dupe, V., Davenne, M., Brocard, J., Dolle, P., Mark, M., Dierich, A., Chambon, P. and Rijli, F. M. (1997). In vivo functional analysis of the Hoxa-1 3′ retinoic acid response element (3′RARE). *Development* **124**, 399-410.
Ensini, M., Tsuchida, T. N., Belting, H. G. and Jessell, T. M. (1998). The control of rostrocaudal pattern in the developing spinal cord: specification of motor neuron subtype identity is initiated by signals from paraxial mesoderm. *Development* **125**, 969-982.
Funaba, M. and Mathews, L. S. (2000). Identification and characterization of constitutively active Smad2 mutants: evaluation of formation of Smad complex and subcellular distribution. *Mol. Endocrinol.* **14**, 1583-1591.
Gamer, L. W., Cox, K. A., Small, C. and Rosen, V. (2001). Gdf11 is a negative regulator of chondrogenesis and myogenesis in the developing chick limb. *Dev. Biol.* **229**, 407-420.
Garces, A., Haase, G., Airaksinen, M. S., Livet, J., Filippi, P. and deLapeyriere, O. (2000). GFRalpha 1 is required for development of distinct subpopulations of motoneuron. *J. Neurosci.* **20**, 4992-5000.
Ge, G., Hopkins, D. R., Ho, W. B. and Greenspan, D. S. (2005). GDF11 forms a bone morphogenetic protein 1-activated latent complex that can modulate nerve growth factor-induced differentiation of PC12 cells. *Mol. Cell. Biol.* **25**, 5846-5858.
Hamburger, V. and Hamilton, H. L. (1951). A series of normal stages in the development of the chick embryo. *J. Morphol.* **88**, 49-92.
Helms, A. W. and Johnson, J. E. (2003). Specification of dorsal spinal cord interneurons. *Curr. Opin. Neurobiol.* **13**, 42-49.
Hollyday, M. (1980a). Organization of motor pools in the chick lumbar lateral motor column. *J. Comp. Neurol.* **194**, 143-170.
Hollyday, M. (1980b). Motoneuron histogenesis and the development of limb innervation. *Curr. Top. Dev. Biol.* **15**, 181-215.
Hollyday, M. and Jacobson, R. D. (1990). Location of motor pools innervating chick wing. *J. Comp. Neurol.* **302**, 575-588.
Jessell, T. M. (2000). Neuronal specification in the spinal cord: inductive signals and transcriptional codes. *Nat. Rev. Genet.* **1**, 20-29.
Kim, J., Wu, H. H., Lander, A. D., Lyons, K. M., Matzuk, M. M. and Calof, A. L. (2005). GDF11 controls the timing of progenitor cell competence in developing retina. *Science* **308**, 1927-1930.
Krumlauf, R., Marshall, H., Studer, M., Nonchev, S., Sham, M. H. and Lumsden, A. (1993). Hox homeobox genes and regionalisation of the nervous system. *J. Neurobiol.* **24**, 1328-1340.
Lance-Jones, C. and Dias, M. (1991). The influence of presumptive limb connective tissue on motoneuron axon guidance. *Dev. Biol.* **143**, 93-110.
Lance-Jones, C., Omelchenko, N., Bailis, A., Lynch, S. and Sharma, K. (2001). Hoxd10 induction and regionalization in the developing lumbosacral spinal cord. *Development* **128**, 2255-2268.
Landmesser, L. (1978a). The development of motor projection patterns in the chick hind limb. *J. Physiol.* **284**, 391-414.
Landmesser, L. (1978b). The distribution of motoneurones supplying chick hind limb muscles. *J. Physiol.* **284**, 371-389.
Lechleider, R. J., Ryan, J. L., Garrett, L., Eng, C., Deng, C., Wynshaw-Boris, A. and Roberts, A. B. (2001). Targeted mutagenesis of Smad1 reveals an essential role in chorioallantoic fusion. *Dev. Biol.* **240**, 157-167.
Lin, A. W. and Carpenter, E. M. (2003). Hoxa10 and Hoxd10 coordinately regulate lumbar motor neuron patterning. *J. Neurobiol.* **56**, 328-337.
Lin, J. H., Saito, T., Anderson, D. J., Lance-Jones, C., Jessell, T. M. and Arber, S. (1998). Functionally related motor neuron pool and muscle sensory afferent subtypes defined by coordinate ETS gene expression. *Cell* **95**, 393-407.
Liu, J. P. and Jessell, T. M. (1998). A role for rhoB in the delamination of neural crest cells from the dorsal neural tube. *Development* **125**, 5055-5067.
Liu, J. P., Laufer, E. and Jessell, T. M. (2001). Assigning the positional identity of spinal motor neurons: rostrocaudal patterning of Hox-c expression by FGFs, Gdf11, and retinoids. *Neuron* **32**, 997-1012.
Lohnes, D. (2003). The Cdx1 homeodomain protein: an integrator of posterior signaling in the mouse. *BioEssays* **25**, 971-980.
Marshall, H., Studer, M., Popperl, H., Aparicio, S., Kuroiwa, A., Brenner, S. and Krumlauf, R. (1994). A conserved retinoic acid response element required for early expression of the homeobox gene Hoxb-1. *Nature* **370**, 567-571.
Massague, J., Seoane, J. and Wotton, D. (2005). Smad transcription factors. *Genes Dev.* **19**, 2783-2810.
Mathis, L. and Nicolas, J. F. (2000). Different clonal dispersion in the rostral and caudal mouse central nervous system. *Development* **127**, 1277-1290.
Mathis, L., Kulesa, P. M. and Fraser, S. E. (2001). FGF receptor signalling is required to maintain neural progenitors during Hensen's node progression. *Nat. Cell Biol.* **3**, 559-566.
McPherron, A. C., Lawler, A. M. and Lee, S. J. (1999). Regulation of anterior/posterior patterning of the axial skeleton by growth/differentiation factor 11. *Nat. Genet.* **22**, 260-264.
Nakashima, M., Toyono, T., Akamine, A. and Joyner, A. (1999). Expression of growth/differentiation factor 11, a new member of the BMP/TGFbeta superfamily during mouse embryogenesis. *Mech. Dev.* **80**, 185-189.
Oh, S. P., Yeo, C. Y., Lee, Y., Schrewe, H., Whitman, M. and Li, E. (2002). Activin type IIA and IIB receptors mediate Gdf11 signaling in axial vertebral patterning. *Genes Dev.* **16**, 2749-2754.
Schoenwolf, G. C. (1992). Morphological and mapping studies of the paranodal and postnodal levels of the neural plate during chick neurulation. *Anat. Rec.* **233**, 281-290.
Shah, V., Drill, E. and Lance-Jones, C. (2004). Ectopic expression of Hoxd10 in thoracic spinal segments induces motoneurons with a lumbosacral molecular profile and axon projections to the limb. *Dev. Dyn.* **231**, 43-56.
Shi, Y. and Massague, J. (2003). Mechanisms of TGF-beta signaling from cell membrane to the nucleus. *Cell* **113**, 685-700.
Shimizu, T., Bae, Y. K., Muraoka, O. and Hibi, M. (2005). Interaction of Wnt and caudal-related genes in zebrafish posterior body formation. *Dev. Biol.* **279**, 125-141.
Sockanathan, S. and Jessell, T. M. (1998). Motor neuron-derived retinoid signaling specifies the subtype identity of spinal motor neurons. *Cell* **94**, 503-514.
Thery, C., Sharpe, M. J., Batley, S. J., Stern, C. D. and Gherardi, E. (1995). Expression of HGF/SF, HGF1/MSP, and c-met suggests new functions during early chick development. *Dev. Genet.* **17**, 90-101.
Tiret, L., Le Mouellic, H., Maury, M. and Brulet, P. (1998). Increased apoptosis of motoneurons and altered somatotopic maps in the brachial spinal cord of Hoxc-8-deficient mice. *Development* **125**, 279-291.
Vermot, J., Schuhbaur, B., Le Mouellic, H., McCaffery, P., Garnier, J. M., Hentsch, D., Brulet, P., Niederreither, K., Chambon, P., Dolle, P. et al. (2005). Retinaldehyde dehydrogenase 2 and Hoxc8 are required in the murine brachial spinal cord for the specification of Lim1+ motoneurons and the correct distribution of Islet1+ motoneurons. *Development* **132**, 1611-1621.
Waldrip, W. R., Bikoff, E. K., Hoodless, P. A., Wrana, J. L. and Robertson, E. J. (1998). Smad2 signaling in extraembryonic tissues determines anterior-posterior polarity of the early mouse embryo. *Cell* **92**, 797-808.
Wichterle, H., Lieberam, I., Porter, J. A. and Jessell, T. M. (2002). Directed differentiation of embryonic stem cells into motor neurons. *Cell* **110**, 385-397.
William, C. M., Tanabe, Y. and Jessell, T. M. (2003). Regulation of motor neuron subtype identity by repressor activity of Mnx class homeodomain proteins. *Development* **130**, 1523-1536.
Wu, H. H., Ivkovic, S., Murray, R. C., Jaramillo, S., Lyons, K. M., Johnson, J. E. and Calof, A. L. (2003). Autoregulation of neurogenesis by GDF11. *Neuron* **37**, 197-207.
Zhang, F., Popperl, H., Morrison, A., Kovacs, E. N., Prideaux, V., Schwarz, L., Krumlauf, R., Rossant, J. and Featherstone, M. S. (1997). Elements both 5′ and 3′ to the murine Hoxd4 gene establish anterior borders of expression in mesoderm and neurectoderm. *Mech. Dev.* **67**, 49-58.
Zimmerman, L., Parr, B., Lendahl, U., Cunningham, M., McKay, R., Gavin, B., Mann, J., Vassileva, G. and McMahon, A. (1994). Independent regulatory elements in the nestin gene direct transgene expression to neural stem cells or muscle precursors. *Neuron* **12**, 11-24.